In press, Journal of Glaciology, 2012

Ice-core net snow accumulation and seasonal snow chemistry at a temperate-glacier site: Mount Waddington, southwest British Columbia, Canada

Peter D. NEFF,[1]* Eric J. STEIG,[1] Douglas H. CLARK,[2] Joseph R. McCONNELL,[3] Erin C. PETTIT,[4] Brian MENOUNOS[5]

[1] Department of Earth and Space Sciences, University of Washington, Seattle, WA, USA 98195
E-mail: neff.peter@gmail.com
[2] Department of Geology, Western Washington University, Bellingham, WA, USA 98225
[3] Division of Hydrologic Sciences, Desert Research Institute, Reno NV, USA 89512
[4] Department of Geology and Geophysics, University of Alaska Fairbanks, Fairbanks, AK, USA 99775
[5] Geography Program, University of Northern British Columbia, Prince George, BC, Canada V2N 4Z9

*Now at Antarctic Research Centre, Victoria University of Wellington, Wellington , New Zealand

ABSTRACT. A 141 m-long ice core was recovered from Combatant Col (51.385°N, 125.258°W, 3000 m a.s.l.), Mount Waddington, Coast Mountains, British Columbia, Canada. Records of black carbon, dust, lead, and water stable-isotopes demonstrate that unambiguous seasonality is preserved throughout the core, despite summer surface snowmelt and temperate ice. High accumulation rates at the site (in excess of 4 m a^{-1} ice-equivalent) limit modification of annual stratigraphy by percolation of surface meltwater. The ice-core record spans the period 1973-2010. An annually-averaged time series of lead concentrations from the core correlates well with historical records of lead emission from North America, and with ice core records of lead from the Greenland Ice Sheet. The depth-age scale for the ice core provides sufficient constraint on the vertical strain to allow estimation of the age of the ice at bedrock. Total ice thickness at Combatant Col is ca. 250 m; an ice-core to bedrock would likely contain ice in excess of 200 years in age. Accumulation at Combatant Col is significantly correlated with both regional precipitation and large-scale geopotential height anomalies.

INTRODUCTION

Numerous ice-core records have been obtained from polar ice sheets and high-altitude tropical glaciers, and are well known for the paleoclimate information they contain (e.g., Thompson and others, 1995; Taylor and others, 1997; Fisher and others, 1998; EPICA, 2004). Ice-core records have also been obtained at mid-latitude sites, which provide information on local sources of anthropogenic and natural aerosols as well as records of regional climate that extend centuries beyond those provided by instrumental records (e.g., Schwikowski and others, 1999; Thompson, 2004; Rupper and others, 2004; Osterberg and others, 2008).

The number of mid-latitude sites suitable for ice cores is limited, and nearly all existing records have been retrieved from just two areas: the coastal ranges of Alaska and the Yukon, and the European Alps. Additionally, a number of records have been developed from lower-latitude sites on the Tibetan Plateau (e.g., Guliya, Dasuopu, Dunde, Thompson, 2000, and Qomolangma, Kaspari and others, 2009), but we do not discuss them here as they more closely resemble polar sites due to extreme high-elevation. North American ice-core sites include the Eclipse Icefield and several sites in the vicinity of Mt. Logan, Yukon (Yalcin and Wake, 2001; Shiraiwa and others, 2003; Fisher and others, 2008), Bona-Churchill Col and Mt. Wrangell, Alaska (Urmann, 2009; Yasunari and others, 2007), and Fremont Glacier, Wyoming (Naftz and others, 1996, 2002). Ice-core sites in the European Alps include Fiescherhorn Glacier (Schwikowski and others, 1999), Colle Gnifetti Glacier (Thevenon and others, 2009), and Col du Dome (Vincent and others, 1997; Preunkert and others, 2000).

Excluding Fremont Glacier, all of these ice-cores were obtained from cold glaciers. Sub-freezing ice temperatures are generally assumed to be essential for preservation of annual stratigraphy; the difficulty of obtaining reliable data from temperate glacier sites is frequently noted in the literature (Naftz and others, 1996; Koerner, 1997; Schotterer and others 1997, 2004; Steig, 2004). For instance, Naftz and others (1996, 2002) retrieved a ~250-year ice-core record from Fremont Glacier (~4000 m a.s.l.) in Wyoming, USA but did not demonstrate the preservation of annual layers. Chemical signals in a ~160 m-long core was retrieved from South Cascade Glacier (~2000 m a.s.l.) in Washington, USA but all chemical signals were even more markedly diffused by meltwater (J. Fitzpatrick, unpublished). As a result of these difficulties, few ice-cores have been obtained from temperate glaciers. Even at sites where the mean annual surface temperature is well below freezing, if summer surface melting occurs, infiltration of meltwater through the snow and firn may compromise or eliminate seasonal stratigraphy. However, once snowfall is transformed through firn to solid glacial ice, little further alteration should be expected, because ice is highly impermeable (Lliboutry, 1971). This suggests that at sites where surface melting occurs, the preservation of annual stratigraphy is primarily controlled by the extent of meltwater infiltration through the firn, rather than the temperature of the ice. Indeed, relatively undisturbed chemical stratigraphy has been observed even at extremely melt-affected sites: in the Lomonosovfonna, Svalbard ice core, where melt presence is reported as high as 80%, only certain acids were affected while isotopes and other chemical species remained immobile (Pohjola and others, 2002; Moore and others, 2005). Ice-cores with intact annual stratigraphy may therefore be retrievable from temperate glaciers, provided the accumulation rate exceeds the infiltration depth. We test this hypothesis in the Coast Mountains of British Columbia, a region characterized by very high precipitation rates and a number of relatively high-elevation sites with ice thicknesses exceeding 200 m. We report results of an ice core from Combatant Col (51.385°N, 125.258°W, 3000 m a.s.l.), which is a broad, nearly flat ice-covered saddle between Mount Waddington and Combatant Mountain in the Waddington Range, southern Coast Mountains (Figures 1 and 2).

ICE-CORE COLLECTION AND ANALYSIS

Ice at Combatant Col diverges and flows through two large icefalls, feeding ice to Tiedemann Glacier to the southeast and Scimitar Glacier to the northwest (Figure 2). A remote weather station maintained by the University of Northern British Columbia, located alongside Tiedemann Glacier 4 km southeast and 1 km below Combatant Col, indicates a mean annual temperature of -5ºC at the ice-core site (assuming a wet adiabatic lapse rate of 7ºC km^{-1}; Peter Jackson, unpublished). Firn temperature measured at 15 m depth also suggests a mean annual temperature of -5ºC (Figure 3c), although this approximation may be of limited use due to the latent heating effect of meltwater (e.g. Pfeffer and Humphrey, 1996)—it may therefore represent an upper limit on mean annual temperature or could simply be a remnant of colder winter temperatures (Paterson, 1994). Radar data collected in 2007 and 2010 indicate an ice thickness of 240 ± 10 m (Figure 3a). Preliminary coring at the site, conducted in September 2006 to a depth of 65 m, suggested high annual accumulation rates, and demonstrated preservation of seasonal cycles in soluble and insoluble chemical species throughout the firn and into the uppermost glacier ice. Data from this preliminary core, however, are discontinuous and thus not of sufficient quality for rigorous comparison to the new record described here (though we do report on water stable-isotope data from the upper 6 m of the 2006 core).

The 141 m Combatant Col ice-core was drilled in July 2010 using the Ice Drilling and Design Office (IDDO) 10-cm diameter electromechanical drill (formerly called the "PICO drill") to a depth of 55 m, and the IDDO 8-cm diameter electrothermal drill from 55 m to 141 m (Ice Drilling Design and Operations, 2011). Thermal drilling became necessary once the presence of water in the borehole prevented evacuation of drill chips in the electromechanical drill sonde. Ice temperature was measured with a thermal probe inserted into a small hole drilled in the side of each core section within 5 minutes of retrieval; ice at the site was between -3ºC and 0ºC at depths below 20 m (Fig. 3c), with consistent temperatures of 0 ± 1ºC below 40 m. The region of transition from cold to temperate ice is clearly visible in the radar stratigraphy at 40 m depth (Figure 3a), likely due to the water-saturated nature of the firn below this depth. The firn-ice transition at 0.83 g cm^{-3} occurs at ~45 m depth (Figure 3b), based on density measured by weighing samples of each ~1 m core section (see below). Freezing of water in the borehole below 80 m depth resulted in partial closure of the borehole over hour- to day-long periods. During one 48-hour drilling shutdown period, for example, a 2 cm-thick annulus of ice developed on the borehole wall. Despite efforts to ensure consistent delivery of ethanol past the porous firn layers and to mix water and ethanol in the borehole, ice freeze-on stalled drilling progress at 118 m. Our attempts to continue drilling required diversion of the borehole at 113.5 m depth, as variance in drill-tower leveling made reopening and following the existing borehole impossible. The divergent borehole, with a deflection of 2-3° from the vertical, reached a final depth of 141 m, after a second diversion at 124 m. We collected overlapping sections of ice at both borehole diversions, in order to recover accurate depth information that was lost when continuous ice-core collection was interrupted. Matching of chemical stratigraphy allowed for recovery of absolute depth correct to within a few centimeters. No further progress could be made below 141 m due to continued refreezing of water in the borehole, leaving ~100 m of ice between the final ice-core depth and the bedrock below.

In the field, we measured, photographed, and placed one-meter ice-core sections into high-density polyethylene (HDPE) bags. The cores were stored in a covered snow pit for up to four days, then taken by a ~30 minute helicopter flight to a freezer truck. At the end of the drilling season, we shipped the ice to storage facilities at the University of Washington in Seattle. In November 2010, we transported the core sections to the U.S. National Ice Core Laboratory in Denver, Colorado for sampling and allocation to laboratories. Core sections were cut into five parallel longitudinal samples: a center core sample (3.5 cm x 3.5 cm x 1 m) for chemical measurements, a side sample for water stable-isotope analysis, and several archive samples. Immediately prior to sampling, a slab of ice from the center of each core section was planed and scanned using a high-resolution digital imaging system (McGwire and others, 2008). We analyzed melt layers in the ice-core by averaging the grayscale pixel intensity of the approximate longitudinal centerline from every core section image taken. This record of pixel intensity clearly demarks transparent, bubble-free melt features as dark horizons, due to the black background and overhead lighting of the imaging system. Melt-free winter snow and firn scatters the overhead lighting and appears bright.

We sampled the ice-core continuously from the surface snow (0 m) to the deepest ice (141 m). Center core samples were analyzed at the Desert Research Institute (DRI) using a continuous-flow system (McConnell and others, 2002; McConnell and others, 2007). In this method, ice samples are melted vertically using a sectioned heating element, isolating the innermost ice from the sample and discarding contaminated outer surfaces. The DRI system employs two high-resolution inductively coupled plasma mass spectrometers for elemental determinations, laser-based instruments for measurements of black carbon and insoluble dust particle concentrations and size distributions, and a range of fluorimeters and spectrophotometers for chemical measurements. This instrumentation yields <1 cm effective depth resolution measurements. Results from the black carbon, lead, and dust measurements, which all exhibit high-amplitude variability throughout the ice core, will be discussed in this paper. Dust data presented here represent particle sizes of 2.4 to 4.5 nm. We also obtained sulfur and acidity measurements, which have been successfully used for the detection of volcanic events at other sites (e.g., Yalcin and others, 2007). Unfortunately the sulfur record provides no evidence of distinct peaks that can be correlated either with known volcanic events or sulfur peaks from other ice-core records in Alaska and the Yukon. Additionally, concerns about contamination of this record in some sections of the core preclude interpretation of any potential events. We measured the density (± 10%) of each 3.5 cm x 3.5 cm x ~1 m core sample, by weighing and measuring dimensions of the ice samples. A density-depth profile estimated from these data using a third-order polynomial fit (Fig. 3b), is used to calculate the ice-equivalent depth and thicknesses of annual-layers in the ice-core.

At the University of Washington stable-isotope laboratory, we cut 1,416 samples at approximately 10 cm resolution for the length of the core, to be used for water stable-isotope ($\delta^{18}O$ and δD) analysis. Each sample was melted, decanted into a 20 mL HDPE bottle, and refrigerated until analysis. Measurements of $\delta^{18}O$ and δD were made simultaneously for each sample using a Picarro cavity ring-down laser spectrometer. We present water stable-isotopes in the classical δ notation as defined by Dansgaard (1964), reporting values relative to Vienna Standard Mean Ocean Water (VSMOW) and normalized to the VSMOW/SLAP scale (e.g. Gonfiantini, 1978).

SEASONALITY IN CHEMICAL RECORDS

Chemical peaks within the Combatant Col ice core, coincident in black carbon, dust, lead and water stable-isotopes, occur in sections of core with higher incidence of melt layers. This relationship is most obvious in the snow and firn portions of the core (0-40 m) where melt-layers are most easily quantified, and chemical peaks do not appear to be preferentially concentrated in individual melt layers. Melt layers in the snow and firn section of the core constitute approximately 7% (~2.8 m) of the total thickness. An example annual sequence is shown in Figure 4. Black carbon concentrations in the core range from 0 to 23.94 parts per billion (ppb) (2.4 ppb standard deviation), while minima typically range from only 0.1 ppb to 1.0 ppb. Dust concentrations range from 0 to 0.68 ppb (0.03 ppb standard deviation), and show several extremely large peaks with concentrations up to 0.4 ppb, while other maxima are as low as 0.05 ppb. Dust minima are less than 0.02 ppb in all cases. The record of lead from Combatant Col ranges from 0 to 2.65 ppb (0.11 ppb standard deviation). Maximum concentrations are observed in the deepest 20 m of the core (121-141 m), with peaks as high as 2 ppb and typical peak values of 0.5 ppb, compared to peak values of $\leq$0.4 ppb in the upper 120 m. Stable-isotope concentrations ($\delta^{18}O$) vary from more negative values (-25‰ to -22‰) in the melt-free portion, to less negative (-18‰ to -14‰) in the melt-rich snow and ice. None of the chemical signals reported here show significant changes in character at or below the firn/ice transition observed at 40-45 m depth, indicating that meltwater alteration of these signals is limited even as they pass through this water-saturated zone.

We interpret the pattern observed in black carbon, dust, and lead measurements as follows. Because maximum precipitation in coastal British Columbia occurs from October to March (1971-2000 climatology; Environment Canada, 2011), we interpret the base of the sequence in Figure 4 as a unit of snow deposited during these winter months. The increasingly impurity-rich upper portion of this snow sequence indicates the gradual addition of impurities to the developing snowpack, coincident with spring and summer months of warmer surface air temperatures and maximum trans-Pacific dust and pollutant fluxes from Asia (Merrill and others, 1989; Bey and others, 2001). Individual trans-Pacific transport events have been observed with diverse compositions; sometimes with components exclusively of industrial origin, though more often they comprise mixes of industrial emission and mineral dust sources (Jaffe and others, 2003). Local contributions of these aerosols are likely also important, considering that a major metropolitan center (Vancouver) is only 280 km distant. Local forest fires may also contribute to the seasonal maximum in black carbon. Finally, occasional storm activity during summer deposits small amounts of snow with high impurity content and less negative $\delta^{18}O$ and δD values. The seasonality in isotopes is consistent with data compiled by Bowen (2008) from the IAEA/WMO Global Network of Isotopes in Precipitation (GNIP) stations and other sources, showing that there is strong seasonality in water isotopes along coastal British Columbia.

Maximum temperatures during summer months (June-August) partially melt surface snow layers—which were deposited in winter and spring—and meltwater from these layers penetrates into the snowpack. Due to exceptionally high accumulation rates at Combatant Col, this meltwater evidently penetrates only part way through an annual-layer. Thus, the seasonal cycle of water stable-isotope values and impurity concentrations is preserved. This interpretation of spring/summer stratigraphic horizon formation is the basis for our annual dating of the ice-core.

DATING

Dating of the core was performed iteratively, by adding independent data sets sequentially after counting subjectively-determined annual peaks. The visual, geochemical and isotope stratigraphy are plotted versus the final age-scale in Figure 5. Initial age-scales were developed using the records of melt layers, black carbon, and dust only. Visual analysis of melt layers was helpful in dating the snow and firn section of the core, showing that closely spaced high-concentration excursions represent individual spring/summer aerosol deposition events (Figure 4, 5a). For depths below 40 m, quantitative visual analysis was not as useful because of reduced contrast between melt layers and melt-free glacier ice (see Figure 5a).

The records of black carbon and dust (Figure 5b, c) provided a preliminary age-scale for the entire core, but there is some ambiguity in certain sections of these records. For this reason, incorporating lead into the dating scheme proved valuable, as extremely low background values of lead provide an independent marker for winter snow (Figure

5d). Additionally, the dated lead time series corresponds well with known histories of lead emissions from North America, giving us confidence in the accuracy of our dating (see below). The significantly elevated lead concentrations in the deepest 20 m of the core correspond with the 1970s, when use of leaded gasoline in the US and Canada was near its maximum. Subsequent regulation by both countries halved the amount of lead in gasoline in 1982, and eliminated it altogether by the early 1990s (Legrand and Mayewski, 1997; Bülhofer and Rosman, 2001). This decrease in lead is clearly observed at Combatant Col, with concentrations sharply dropping off in the early 1980s and remaining low through the 1990s.

We compare the lead records from four sites: Combatant Col (Figure 6a), southwest Greenland ACT2 (Figure 6a; McConnell and Edwards, 2008), Greenland Summit (Figure 6a; J. McConnell, unpublished), and Mt. Logan Prospector-Russell Col (Figure 6b; Osterberg and others, 2008). The Combatant Col lead record correlates well with both the Greenland ACT2 and Greenland Summit lead records, at greater than 95% significance (see Table 1). All significance levels presented account for autocorrelation following Bretherton and others (1999). Lead-isotope data indicate that North America is the dominant source of lead in Greenland (Rosman and others, 1994). That the Combatant Col lead record compares favorably with Greenland suggests that that lead aerosol deposited at Combatant Col is primarily North American in source, and also indicates our dating of the ice core is accurate. The Combatant Col lead record shows no significant correlation with that of Mt. Logan, where large peaks in lead concentration are observed during the 1980s, and increasing concentrations are observed up to the most recent years of the record (see Figure 6 and Table 1). This history of lead deposition at Mt. Logan has been interpreted as largely of Asian origin, due to later industrialization and less stringent regulation of pollution than in North America (Osterberg and others, 2008).

Water stable-isotopes, $\delta^{18}O$ and δD, were the final component included in our multi-parameter dating of the Combatant Col ice core. For the purposes of dating, $\delta^{18}O$ and δD are nearly identical, so we report only $\delta^{18}O$ here (Figure 5e). The initial time scales, based on visual and chemical stratigraphy only, agree well with the $\delta^{18}O$ data. Due to the thick annual layers at Combatant Col, the relatively coarse 10 cm sampling for water stable-isotope measurements results in an average of 35 samples per year. Data from surface snow and firn cores drilled at the site in 2006 provide additional, definitive validation for our dating of the most recent five years of the 2010 ice core (see Figure 7). In the 2006 core, the top of which represents the snow surface during summer of that year, we see anomalously negative $\delta^{18}O$ values (-30‰) 2.3 m below the surface, deposited during winter 2005-2006 or spring 2006. This same 2006 annual-layer from the more recent and longer Combatant Col ice core, now buried at a depth of ~36 m, exhibits nearly identical minimum values—the most negative of the entire record. We are confident that these are the same annual-layer, and we further note that the $\delta^{18}O$ values are well-preserved at depth, showing no evidence of alteration of the original surface layers deposited in 2006 through the subsequent four years. This finding is significant, because alteration of water stable-isotopes, including diminished seasonality and an overall decrease in summertime values, is commonly observed even at cold glacier sites (e.g. Koerner, 1997; Moran and Marshall, 2009). In the Combatant Col core, we observe seasonal isotope variation of roughly constant amplitude throughout the record, including in the deepest ice.

ANNUAL-LAYER THICKNESS AND ICE-FLOW CORRECTIONS

Annual-layer thicknesses from the Combatant Col ice core (Figure 8) indicate extremely thick snow and ice sequences from the most recent (and least flow-altered) layers at the site, up to 12 m at the thickest (~8.3 m, ice-equivalent). These layers gradually thin with depth, due to ice-flow, to reach annual-layer thicknesses of 1-2 m ice-equivalent at depths below ~100 m. We calculate uncertainties in layer thickness by considering the standard error of the thicknesses from four sequentially developed age scales.

To obtain annual accumulation rates, we correct annual layer thicknesses for dynamic thinning using the one-dimensional ice-flow model of Dansgaard and Johnsen (1969). This model uses a simple piecewise-linear approximation of the horizontal-velocity profile, assumed to be constant at value u_s from the surface down to some distance h above the bed, and then decreasing linearly towards a value u_b, which is the sliding velocity, at the bed. The depth-age relation for constant accumulation and steady state flow is given as follows, where H is the total ice thickness, $\dot{b}$ is the surface accumulation rate, u_s is the surface velocity, and z is the distance above the bed.

$$t(z) = \frac{H}{u_s \dot{b}} \left(\ln \frac{h(u_b - u_s) + 2u_s z}{h(u_b - u_s) + 2u_s} \right) \qquad z > h$$

$$t(z) = \frac{2H}{u_s \dot{b}} \ln \left(\frac{(u_b - u_s)h + 2u_s h}{(u_b - u_s)h + 2u_s} \right) \qquad z = h$$

$$t(z) = t(h) + \frac{H}{u_b \dot{b}} \left(\ln \frac{z}{(u_b - u_s)z - 2u_b h} - \ln \frac{h}{(u_b - u_s)h - 2u_b h} \right) \qquad z < h,\ u_b > 0$$

$$t(z) = \frac{2H}{u_s \dot{b}} \left(1 - \frac{h}{z} \right) \qquad z < h,\ u_b = 0$$

Assuming that there is no long-term trend in accumulation rate—no significant trends are observed in regional weather station precipitation records (Environment Canada, 2011) during the time period overlapping with the ice core record,—we can estimate the parameter h and the ratio u_b/u_s by minimizing the difference between the calculated and observed age-depth relationship over a range of plausible values of surface accumulation rate $\dot{b}$ and total ice thickness, H. That is, we minimize the root mean square difference $\sqrt{\sum \left(t_m(z) - t(z)\right)^2}$ where t_m is the measured timescale and t is the calculated timescale at ice-equivalent heights z (Figure 9a). Note that although it is virtually certain that there is melting at the bed, it is negligible in this setting even at very high geothermal heat flux, because the surface accumulation rate is so high. For example, a geothermal heat flux of 120 mW m^{-2}, about twice the regional average (e.g. Lewis and others, 1985), would result in basal melt rates of order only 1 cm a^{-1} (e.g. Paterson, 1994).

The results show that lowest *rms* values are found with $\dot{b}$ ~ 7 m a^{-1} and H ~ 240 m (ice equivalent), both consistent with the observations. Optimal values of h/H and u_b/u_s

are h/H ~ 0.6-0.7, $u_b/u_s < 0.1$ (Figure 9a), consistent with typical values for flow near an ice divide (Waddington and others, 2001). We note that somewhat lower *rms* values can be obtained for $\dot{b}$ = 8 m a^{-1} and H = 260 m, if h/H is >0.9. However, H > 250 m is unlikely on the basis of the radar data (Figure 3a). Basal sliding rates greater than u_b/u_s = 10% would also require ice thicknesses that are likely ruled out by the radar data, strongly indicating that basal sliding is a small fraction of the total sliding. In any case, corrections to the annual layer thickness using a range of plausible choices are essentially identical to those for $\dot{b}$ = 7 m a^{-1} and H = 240 m, because higher accumulation rates and/or high sliding rates require greater thinning at depth (and therefore a greater value of h/H) to be consistent with the observations. Conversely, low values of accumulation rate imply smaller values of H and h/H. However, depths <230 m are inconsistent with the observed depth-age relationship, regardless of the values of h/H and u_b/u_s used. We conclude that the observed depth-age relationship strongly constrains the layer-thinning profile with depth, allowing us to convert the measured layer thicknesses to original annual accumulation rates at the surface. For simplicity, we use $\dot{b}$ = 7 m a^{-1}, $h/H = 0.65$, H = 240 m, and $u_b/u_s = 0$. Figure 9b compares the calculated timescale for these parameters with the observed depth-age profile from the Combatant Col ice core. Note that the implied age at depth is well in excess of 200 years; we discuss the implications of this for future work later in this paper.

The time series of ice flow-corrected net annual accumulation from Combatant Col is shown in Figure 10. We estimate uncertainty in the accumulation data by taking into account the estimated uncertainty in the timescale, based on the sequence of four depth-age relationships developed iteratively as individual stratigraphic time series (i.e. records of melt layers, geochemistry, isotopes) were incorporated into our multiparameter dating (described in "Dating" section above). This translates to an average uncertainty of ~12% in accumulation for each year, or, equivalently, an age uncertainty of ~1 year. Maximum annual accumulation rates of 10-11 m a^{-1} ice-equivalent are observed, with minima no lower than ~4 m a^{-1}. Annual accumulation rates of this magnitude, averaging 6.8 m a^{-1} over this 38-year record, place Combatant Col among the wettest places on the planet (see National Climatic Data Center, 2008). In contrast, lee-ward climate stations on Vancouver Island only average annual precipitation of 1.0-1.5 m a^{-1} from 1971-2000 (Environment Canada, 2011).

RELATIONSHIP BETWEEN ACCUMULATION RATE AND REGIONAL PRECIPITATION

Time series of annual snow accumulation developed from alpine ice core records have been used previously as indicators of past climate variability. A central challenge to using ice core records in this way, however, is that the accumulation rate at a specific high-altitude site may reflect only very regional climate, or even microclimatic conditions. Nevertheless, previous studies have had some success: the Mt. Logan accumulation time-series has been used to examine variability in the strength of the Aleutian Low (e.g. Moore and others, 2003), while Rupper and others (2004) argued that the Mt. Logan record could be meaningfully related to the large-scale precipitation variability for the largest winter storms. It is therefore of interest to examine the extent to which the Combatant Col record may similarly reflect regional or large-scale climate variability.

Comparison with both local precipitation records (locations marked in Figure 1 and detailed in Table 2) and large-scale climate reanalyses suggests that the Combatant Col record does meaningfully reflect regional-scale precipitation. We calculated the correlation between the annually-averaged accumulation from Combatant Col and the annually-averaged precipitation rates from British Columbia weather stations (Environment Canada, 2011), using seasonal (3-month) averages for all seasons, starting in July (the nominal beginning of each accumulation year in the core), for lags of up to one year. We find that correlations are maximized with a lag of one year, and are significant at that lag ($p < 0.05$). Although a lag of one year is obviously not physically meaningful, this lies within the expected dating uncertainty for the core. Several lines of evidence argue the high correlations reflect a real, physically meaningful relationship between Combatant Col accumulation and regional precipitation. First, the maximum correlation occurs when the station averages are centered on the winter accumulation season, November through January. Second, more significant correlations are found with weather station precipitation records on the windward (west) side of the Coast Mountains, at Port Hardy, Tofino, and Campbell River on Vancouver Island, plus Powell River on the mainland. Stations east of the range's crest or further north (Tatlayoko, Lillooet, Bella Coola, and Prince Rupert) show correlations in some seasons but are less consistent in timing and in general are less significant. The pattern of greater correlation with stations to the west is to be expected, because Mt. Waddington clearly receives precipitation almost exclusively due to orographic effects as westerly storms encounter the Coast Mountains, rather than from easterly flow originating in the dry British Columbia interior.

We find that if we shorten the total length of the record by one year, by combining the annual accumulation total of two adjacent years—a reasonable possibility as annual stratigraphy in some years is not entirely unambiguous—significant correlations remain, but with zero lag. The most likely candidate pair of years is 2004 and 2005. The spring/summer chemical peak originally selected as the lower/older boundary of year 2005 is ambiguous (see Figure 5). This adjustment yields a very high accumulation rate estimate for 2005 (i.e.. the 5.9 m in 2004 and 7.4 m in 2005 becomes 13.3 m ice-equivalent in 2005), in agreement with weather station precipitation data from coastal weather station sites southwest (upwind) of Combatant Col (e.g. Tofino; Environment Canada, 2011). Further, the seasonal correlation using this timescale remains maximized in November though January, consistent with the climatological maxima in both precipitation amount and precipitation variability (Figure 11, Table 3).

In Figure 12, we compare the annual mean Combatant Col time series with large-scale precipitation and atmospheric circulation variability using annual precipitation and geopotential height data (averaged July through June) from the ERA40/ERA-Interim climate reanalysis data (Upalla and others, 2005; Dee and others, 2011). We find significance levels are high where expected: over Mt. Waddington itself, and over Vancouver Island to the immediate west (Figure 12a). Furthermore, the correlation pattern with both precipitation and 500 hPa geopotential heights is consistent with previous understanding of large-scale controls on precipitation variability in this region (Overland and Hiester, 1980). In particular, positive correlations with precipitation extend westward along the climatological trajectory of westerly wind, while there is a negative correlation with precipitation in coastal Alaska, similar to the characteristic South-North dipole pattern associated with the Pacific/North American pattern (Wallace and Gutzler, 1981). The correlation with 500 hPa geopotential height is strongly negative (associated with lower than average geopotential heights) over the Gulf of Alaska. This is a similar configuration of geopotential height to that associated with greater than average storminess and precipitation along the west coast of British Columbia (Rodionov and others, 2007).

These correlations are based on a relatively short record, only 37 years, while the ultimate goal of this ice-core project is to gain insight into regional conditions extending beyond the instrumental period. This should be achievable at Combatant Col, because the presence of ice in excess of 200 years near the bed is very likely based on observed depth-age relationship. A longer record should also allow for more precise dating, because the age of deeper ice would likely be constrained by deposits from the Katmai, Alaska (1912), Tambora, Indonesia (1815), and other eruptions seen in the Eclipse Icefield and Mount Logan ice cores (Yalcin and others, 2007).

CONCLUSIONS

Retrieving ice-core paleoclimate records from temperate glaciers has been attempted only rarely, because it has often been observed that annual stratigraphy—critical to dating the records—will not be preserved. Our results from the Combatant Col ice core demonstrate that unambiguous seasonal stratigraphy can be preserved in visual and chemical records from temperate ice, provided that annual snow accumulation rates exceed the depth penetrated by summer surface meltwater. In addition to allowing for accurate dating, preserved chemical stratigraphy provides valuable information about the deposition of natural and anthropogenic aerosols at remote sites. The record of lead deposited at Combatant Col likely reflects a North American source since the 1970s, correlating well with North American lead-emission histories and with lead records from Greenland ice cores. This contrasts with the Asian source of lead deposited at Mt. Logan, and illustrates the value of exploiting ice core records from mid-latitude sites, which clearly do not reflect the same atmospheric circulation as more northerly locations. Furthermore, based on its covariance with regional weather station and climate reanalysis data the accumulation time series from the Combatant Col ice core appears to meaningfully reflect regional-scale climate variability. These results suggest that there is more potential than previously thought in exploring ice-core sites at mid-latitudes where cold glaciers are uncommon. Although the high-accumulation criterion limits the age of ice preserved at depth in relatively shallow alpine glaciers, ice with an age of several hundreds of years is likely preserved at Combatant Col. Because of Combatant Col's location at the southern extreme of the dipole pattern in precipitation along the coast of northwestern North America (e.g. Bitz and Battisti, 1999), information from a deeper ice-core at this site would add important spatial detail to the study of regional climate variability using existing records from Alaska and the Yukon.

ACKNOWLEDGEMENTS

We thank Beth Bergeron and Ice Drilling Design and Operations for expert drilling leadership, the King family and employees at White Saddle Air, Bluff Lake, British

Columbia, and TC Trans trucking for an emergency ice-core freezer replacement. Field assistants were M. Bisiaux, N. Bowermann, K. Sterle, J. Theis, S. Schoenemann, A. McKee, M. Park, T. Hutchison, J. Brann and K. McConnell. H. Roop assisted in planning field logistics, and helped process the core along with A. Gusmeroli. T.J. Fudge assisted in dating of the core. We also thank the National Ice Core Laboratory for sampling support, and technicians and students at the Desert Research Institute Ultra-Trace Chemistry Laboratory and Andrew Schauer and other staff at Δ*IsoLab (University of Washington) for their analytical expertise. We thank E.D. Waddington, G. Roe, M. Winstrup, and two anonymous reviewers for providing helpful comments on the manuscript. This project was supported by grants from the U.S. National Science Foundation Paleoclimate Program, award numbers 0902240, 0902392, 0902734, and 0903124, and by the Western Canadian Cryospheric Network, funded by the Canadian Foundation for Climate and Atmospheric Sciences.

REFERENCES

Bey I and 3 others (2001) Asian chemical outflow to the Pacific in spring: Origins, pathways, and budgets. *J. Geophys. Res.*, **106**, D000806. (0148-0227/01/2001JD000806.)

Bitz CM and Battisti DS (1999) Interannual to decadal variability in climate and the glacier mass balance in Washington, western Canada, and Alaska. *J. Clim.*, **12**, 3181-3196.

Bowen GJ (2008) Spatial analysis of the intra-annual variation of precipitation isotope ratios and its climatological corollaries. *J. Geophys. Res.*, **113**, D05113. (10.1029/2007JD009295)

Bretherton CS and 4 others (1999) The effective number of spatial degrees of freedom of a time-varying field. *J. Clim.*, **12**(7), 1990-2009.

Bulhöfer A and Rosman KJR (2001) Isotopic source signatures for atmospheric lead: The Northern Hemisphere. *Geochim. Cosmochim. Acta*, **65**(11), 1727-1740.

Dansgaard W (1964), Stable isotopes in precipitation, *Tellus*, **16**(4), 436–468,

doi:10.1111/j.2153-3490.1964.tb00181.x.
Dansgaard W and Johnsen SJ (1969) A flow model and a time scale for the ice core from Camp Century, Greenland. *J. Glaciol.*, **8**(53), 215–223.
Dee DP and 35 others (2011) The ERA-Interim reanalysis: configuration and performance of the data assimilation system. *Q. J. R. Meteorol. Soc.*, **137**, 553-597. DOI:10.1002/qj.828
Environment Canada (2011) Canadian climate normals 1971-2000. *National Climate Data and Information Archive*. www.climate.weatheroffice.gc.ca.
EPICA community members (2004) Eight glacial cycles from an Antarctic ice core. *Nature*, **429**, 623-628.
Fisher DA and 12 others (1998) Penny Ice Cap cores, Baffin Island, Canada, and the Wisconsinan Foxe Dome connection: two states of Hudson Bay ice cover. *Science*, **279** (5351), 692-695.
Fisher DA and 16 others (2008) The Mt Logan Holocene-late Wisconsinan isotope record: tropical Pacific-Yukon connections. *The Holocene*, **18**(5), 667-677.
Gonfiantini, R. 1979. Standards for stable isotope measurements in natural compounds. *Nature,* 271(5645), 534-536.
Ice Drilling Design and Operations (2011) *Long Range Drilling and Technology Plan*. University of Wisconsin, Madison. Ice Drilling Program Office. http://icedrill.org/documents/view.shtml?id=272.
Jaffe D and 3 others (2003) Six 'new' episodes of trans-Pacific transport of air pollutants. *Atmos. Envir.,* **37**(3), 391-404.
Kaspari S and 7 others (2009) A high-resolution record of atmospheric dust composition and variability since A.D. 1650 from a Mount Everest ice core. *J. Clim.*, 22, 3910-3925.
Koerner RM (1997) Some comments on climatic reconstructions from ice cores drilled in areas of high melt. *J. Glaciol.*, **43**(143), 90-97.
Legrand M and Mayewski P (1997) Glaciochemistry of polar ice cores: a review. *Rev. Geophys.*, **35**(3), doi:10.1029/96RG03527.
Lewis TJ, Jessop AM and Judge AS (1985) Heat flux measurements in southwestern British Columbia: the thermal consequences of plate tectonics. *Canadian Journ. of Earth Sci.*, **22**(9), 1262-1273.
Lliboutry L (1971) Permeability, brine content and temperature of temperate ice. *J. Glaciol.*, **10**(58), 15-29.
McConnell JR and 3 others (2002) Continuous ice-core chemical analyses using inductively coupled plasma mass spectrometry. *Envir. Sci. Technol.*, **36**(1), 7-11.
McConnell JR and 9 others (2007) 20th-century industrial black carbon emissions altered Arctic climate forcing. *Science*, **317**, 1381-1384.
McConnell JR and Edwards R (2008) Coal burning leaves toxic heavy metal legacy in the Arctic. *Proceedings of the National Academy of Sciences*, doi:10.1073/pnas.0803564105
McGwire KC and 6 others (2008) An integrated system for optical imaging of ice cores. *Cold Reg. Sci. Technol.*, **53**(2), 216-228.

Merrill JT, Uematsu M and Bleck R (1989) Meterological analysis of long range transport of mineral aerosols over the North Pacific. *J. Geophys. Res.*, **94**, D00089. (0148-0227/89/89JD00089.)

Moore GWK, Holdsworth G and Alverson K (2003) The impact that elevation has on the ENSO signal in precipitation records from the Gulf of Alaska. *Climatic Change,* **59** (1–2), 101–121.

Moore JC and 3 others (2005) Separation of melting and environmental signals in an ice core with seasonal melt. *Geophys. Res. Lett.*, **32**, L10501, doi:10.1029/2005GL023039.

Moran T and Marshall S (2009) The effects of meltwater percolation on the seasonal isotopic signals in an Arctic snowpack. *J. Glaciol.*, **55**(194), 1012-1024.

Naftz DL and 7 others (1996) Little Ice Age evidence from a south-central North American ice core, U.S.A. *Arc. and Alp. Res.*, **28**(1), 35-41.

Naftz DL and 6 others (2002) Ice core evidence of rapid air temperature increases since 1960 in alpine areas of the Wind River Range, Wyoming, United States. *J. Geophys. Res.*, **107**(D13), 10.1029/2001JD000621.

National Climatic Data Center (2008) Global measured extremes of temperature and precipitation. *U.S. Dept. of Commerce*. http://www.ncdc.noaa.gov/oa/climate/globalextremes.html#sites. Accessed March 1, 2012.

Osterberg E and 10 others (2008) Ice core record of rising lead pollution in the North Pacific atmosphere. *Geophys. Res. Lett.*, **35**, L05810. (10.1029/2007GL032680.)

Overland JE and Hiester TR (1980) Development of a synoptic climatology for the Northeast Gulf of Alaska. *J. Appl. Met.*, **19**(1), 1-14.

Paterson WSB (1994) *The Physics of Glaciers*, 3rd ed., 481pp., Elsevier, Amsterdam.

Pfeffer WT and Humphrey NF (1996) Determination of timing and location of water movement and ice-layer formation by temperature measurements in sub-freezing snow. *J. Glaciol.*, **42**(141), 292-304.

Pohjola VA and 7 others (2002) Effect of periodic melting on geochemical and isotopic signals in an ice core from Lomonosovfonna, Svalbard. *J. Geophys. Res.*, 107(D4), 4036, doi: 10.1029/2000JD000149.

Preunkert S and 3 others (2000) Col du Dôme (Mont Blanc Massif, French Alps) suitability for ice-core studies in relation with past atmospheric chemistry over Europe. *Tellus*, **52B**, 993-1012.

Rodionov SN, Bond NA and Overland JE (2007) The Aleutian Low, storm tracks, and winter climate variability in the Bering Sea. *Deep Sea Res. II*, **54**, 2560-2577.

Rosman KJR and 4 others (1994) Isotopic evidence to account for changes in the concentration of lead in Greenland snow between 1960 and 1988. *Geochim. Cosmochim. Acta*, **58**(15), 3265-3269.

Rupper S, Steig EJ and Roe G (2004) The relationship between snow accumulation at Mt. Logan, Yukon, Canada, and climate variability in the North Pacific. *J. Climate*, **17**(24), 4724-4739.

Schotterer U and 3 others (1997) Isotope records from Mongolian and Alpine ice cores as climate indicators. *Climatic Change*, **36**, 519-530.

Schotterer U, Stichler W and Ginot P (2004) The influence of postdepositional effects on ice core studies: examples from the Alps, Andes, and Altai. *In* Cecil, L.D., J.R. Green and L.G. Thompson, *eds. Earth paleoenvironments: records preserved in mid- and low-latitude glaciers*. Dordrecht, etc., Kluwer Academic, 39-60.

Schwikowski M and 3 others (1999) A high-resolution air chemistry record from an Alpine ice core: Fiescherhorn glacier, Swiss Alps. *J. Geophys. Res.*, **104**, D100112. (0148-0227/99/1998JD100112).

Shiraiwa T and 7 others (2003) Ice core drilling at King Col, Mount Logan 2002. *Bull. Glaciol. Res.*, **20**, 57-63.

Steig EJ (2004) Foreword. *In* Cecil LD, Green JR, Thompson LG, *eds. Earth Paleoenvironments: records preserved in mid- and low-latitude glaciers*. Dordrecht, etc., Kluwer Academic, xxix-xxix.

Taylor KC and 12 others (1997) The Holocene-Younger Dryas transition recorded at Summit, Greenland. *Science*, **278**, 825-827.

Thevenon F and 3 others (2009) Mineral dust and elemental black carbon records from and Alpine ice core (Colle Gnifetti glacier) over the last millennium. *J. Geophys. Res.*, **114**, D17102. (10.1029/2008JD011490).

Thompson LG and 7 others (1995) Late Glacial Stage and Holocene tropical ice core records from Huascarán, Peru. *Science*, **269**(5220), 46-50.

Thompson LG (2000) Ice core evidence for climate change in the Tropics: implications for our future. *Quat. Sci. Rev.*, **19**, 19-35.

Thompson LG (2004) High-altitude, mid and low-latitude ice core records: implications for our future. *In* Cecil LD, Green JR and Thompson LG, *eds. Earth paleoenvironments: records preserved in mid- and low-latitude glaciers*. Dordrecht, etc., Kluwer Academic, 3-15.

Uppala SM and 45 others (2005) The ERA-40 re-analysis. *Q. J. R. Meteorol. Soc.*, **131**, 2961-3012. DOI: 10.1256/qj.04.176

Urmann D (2009) Decadal scale climate variability during the last millennium as recorded by the Bona Churchill and Quelccaya ice cores. PhD thesis, Ohio State University, Columbus.

Vincent C and 4 others (1997) Snow accumulation and ice flow at Dôme du Goûter (4300m), Mont Blanc, French Alps. *J. Glaciol.*, **43**(145), 513-521

Waddington ED, Bolzan JF and Alley RB (2001) Potential for stratigraphic folding near ice-sheet centers. *J. Glaciol.,* **47**(159), 639-648.

Wallace JM and Gutzler DS (1981) Teleconnections in the geopotential height field during the Northern Hemisphere Winter. *Mon. Wea. Rev.*, **109**, 784-812.

Yalcin K and Wake CP (2001) Anthropogenic signals recorded in an ice core from Eclipse Icefield, Yukon Territory, Canada. *Geophys. Res. Lett.,* **28**(23), 4487-4490.

Yalcin K and 4 others (2007) Ice core paleovolcanic records from the St. Elias Mountains, Yukon, Canada. *J. Geophys. Res.*, **112**, D08102. (10.1029/2006JD007497).

Yasunari TJ and 7 others (2007) Intra-annual variations in atmospheric dust and tritium in the North Pacific region detected from an ice core from Mount Wrangell, Alaska. *J. Geophys. Res.*, **112**, D10208. (10.1029/2006JD008121.)

TABLES

Table 1. Correlation (*r*) and significance (*p*) between annual Combatant Col lead record and other ice core lead records. Correlations with >95% significance are in bold.

Ice core	Coordinates	Elevation (m a.s.l.)	Record length (used in correlations)	Combatant Col Pb correlation (*r*)	Significance (*p*)
ACT2	66.0ºN, 45.2ºW	2410	1973-2002	**0.82**	**<0.02**
Summit	72.6°N, 38.5°W	3210	1973-2009	**0.62**	**<0.02**
Mount Logan (PR Col)	60.6°N, 140.6°W	5300	1973-1998	-0.25	0.21

Table 2. Coordinates, elevation, and record lengths for all Environment Canada weather stations used in precipitation-accumulation correlations.

Location	Coordinates	Elevation (m a.s.l.)	Record length (used in correlations)
Port Hardy	50.68ºN, 127.37ºW	21.6	1973-2009
Powell River	49.88ºN, 124.55ºW	51.8	1973-2006
Campbell River	49.95ºN, 125.27ºW	105.5	1973-2006
Tofino	49.08ºN, 125.77ºW	24.5	1973-2006
Bella Coola	52.37ºN, 126.69ºW	18.3	1973-2002
Prince Rupert	54.29ºN, 130.44ºW	35.4	1973-2005
Lilloet	50.67ºN, 121.92ºW	198.1	1973-2000
Tatlayoko	51.67ºN, 124.41ºW	870	1973-1997

Table 3. Correlation (*r*) and significance (*p*) between the annual mean Combatant Col accumulation time series (1973.5-2009.5), adjusted by 1-year as detailed in the text, and precipitation at Environment Canada weather stations for different 3-month averages (beginning March 1973) and annual mean (averaged July through June). MAM = March April May, MJJ = May June July, JAS = July August September, SON = September October November, NDJ = November December January, JFM = January February March. Bold numbers show where positive correlations are significant at better than $p < 0.1$, with $p<0.05$ in italics.

Location	**MAM**		**MJJ**		**JAS**		**SON**		**NDJ**		**JFM**		**Annual**	
	r	***p***	***r***	***p***	***r***	***p***	***r***	***p***	***r***	***p***	***r***	***p***	***r***	***p***
Port Hardy	0.05	0.73	-0.19	0.21	0.13	0.40	***0.32***	***0.03***	***0.57***	***0.00***	***0.34***	***0.02***	***0.59***	***0.00***
Powell River	-0.16	0.32	-0.21	0.18	0.14	0.38	0.20	0.19	***0.50***	***0.00***	**0.25**	**0.10**	***0.41***	***0.01***
Campbell River	0.00	0.99	-0.18	0.26	0.12	0.46	***0.34***	***0.03***	**0.28**	**0.07**	0.01	0.95	0.23	0.14
Tofino	-0.09	0.55	-0.19	0.22	0.10	0.53	**0.30**	**0.05**	***0.59***	***0.00***	***0.34***	***0.03***	***0.61***	***0.00***
Bella Coola	0.13	0.43	0.21	0.22	-0.01	0.98	0.21	0.22	**0.32**	**0.06**	-0.03	0.88	0.18	0.29
Prince Rupert	-0.01	0.94	-0.08	0.60	0.08	0.62	0.04	0.80	-0.10	0.53	-0.06	0.70	-0.06	0.72
Lillooet	-0.16	0.37	-0.19	0.29	-0.09	0.63	**0.32**	**0.06**	***0.38***	***0.03***	***0.48***	***0.01***	0.12	0.50
Tatlayoko	***0.44***	***0.01***	-0.08	0.67	-0.35	0.05	0.04	0.82	***0.43***	***0.02***	-0.02	0.93	-0.17	0.38

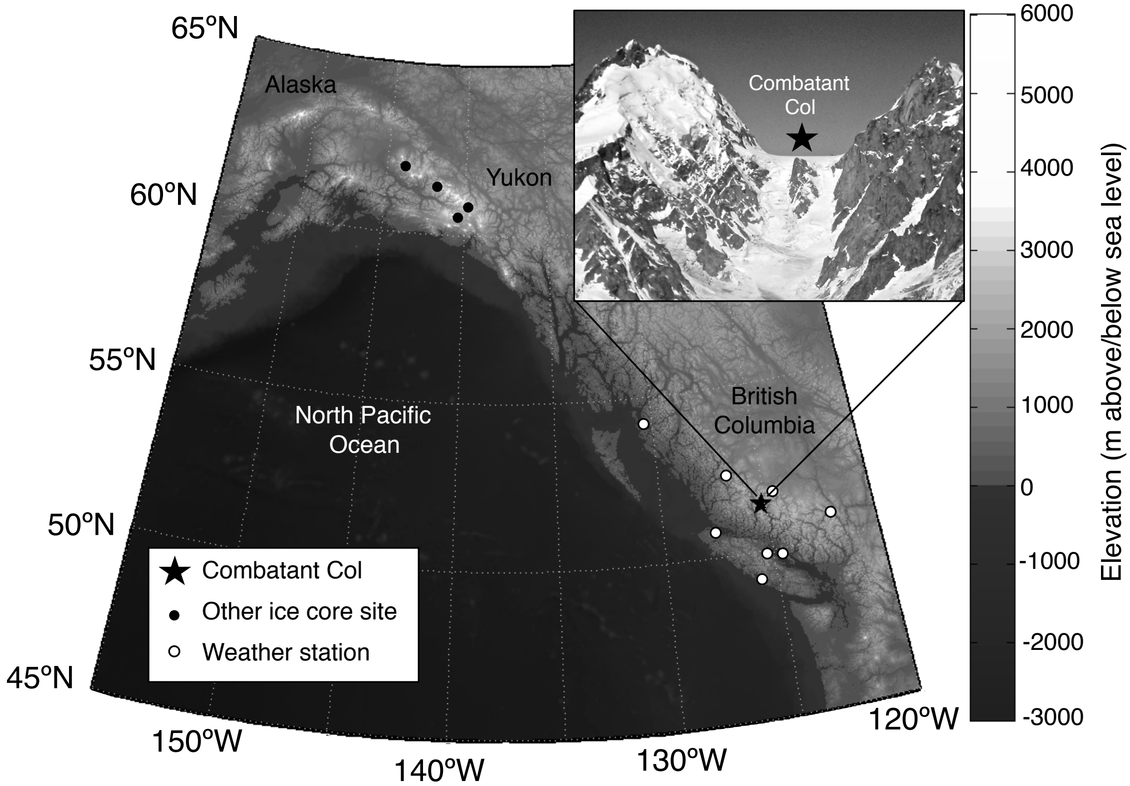

Figure 1. Map location of Combatant Col drill site (starred), with inset picture showing local setting (E. Steig photo). Other ice cores and weather stations mentioned in the text are marked by black and white circles, respectively.

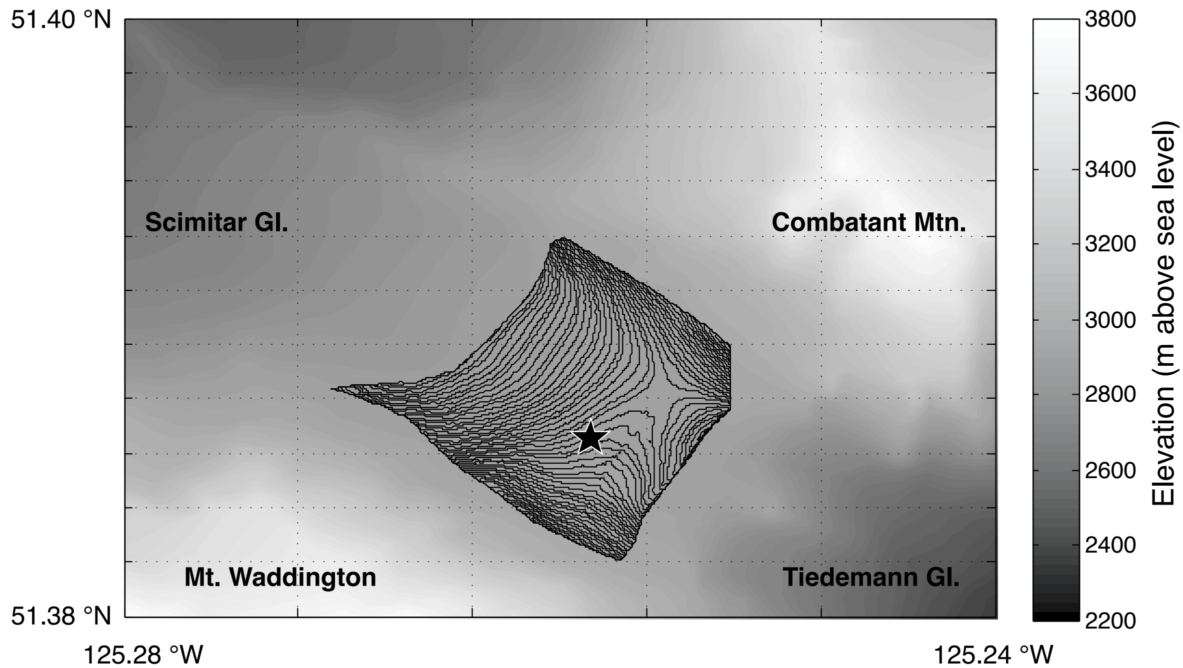

Figure 2. Drill site (starred) detail and ice-surface topography. Grayscale shading derived from 20 m digital-elevation map (DEM) data. Black contours are derived from GPS surveys conducted during field campaigns and are plotted with a 2 m contour interval. These new surface-elevation data correct 20-40 m errors in the original 20 m DEM at Combatant Col.

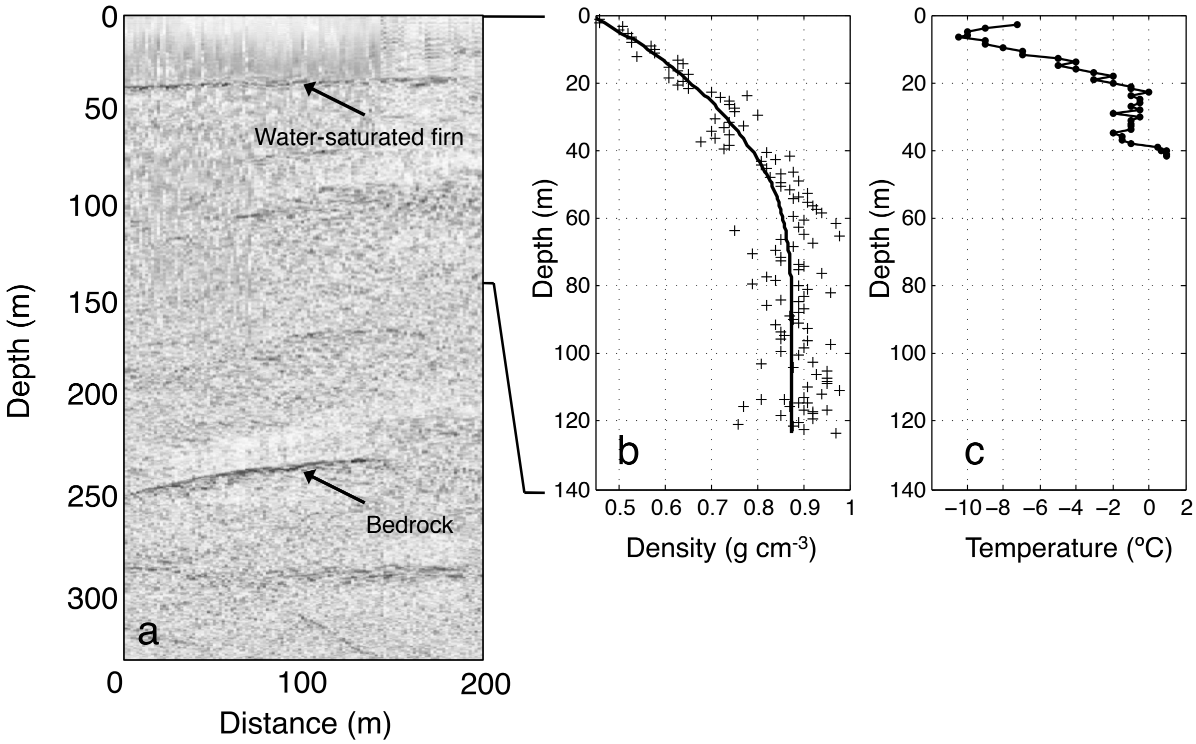

Figure 3. a) Radar data (80 MHz center frequency) from a 200 m transect across the Combatant Col drill site, trending roughly along the ice flow-divide (southwest to northeast). Arrows indicate the location of water-saturated firn, near 40 m depth, and a bedrock reflector at ~250 m. b) Ice-core density measurements, made in the laboratory, fit with a 3rd-order polynomial used to calculate ice-equivalent depths. The firn-ice transition at 0.83 g cm^{-3} occurs at a depth of ~45 m. c) Ice-core temperature, measured in the field, shows ice reaching ~0 ºC at a depth of 40 m.

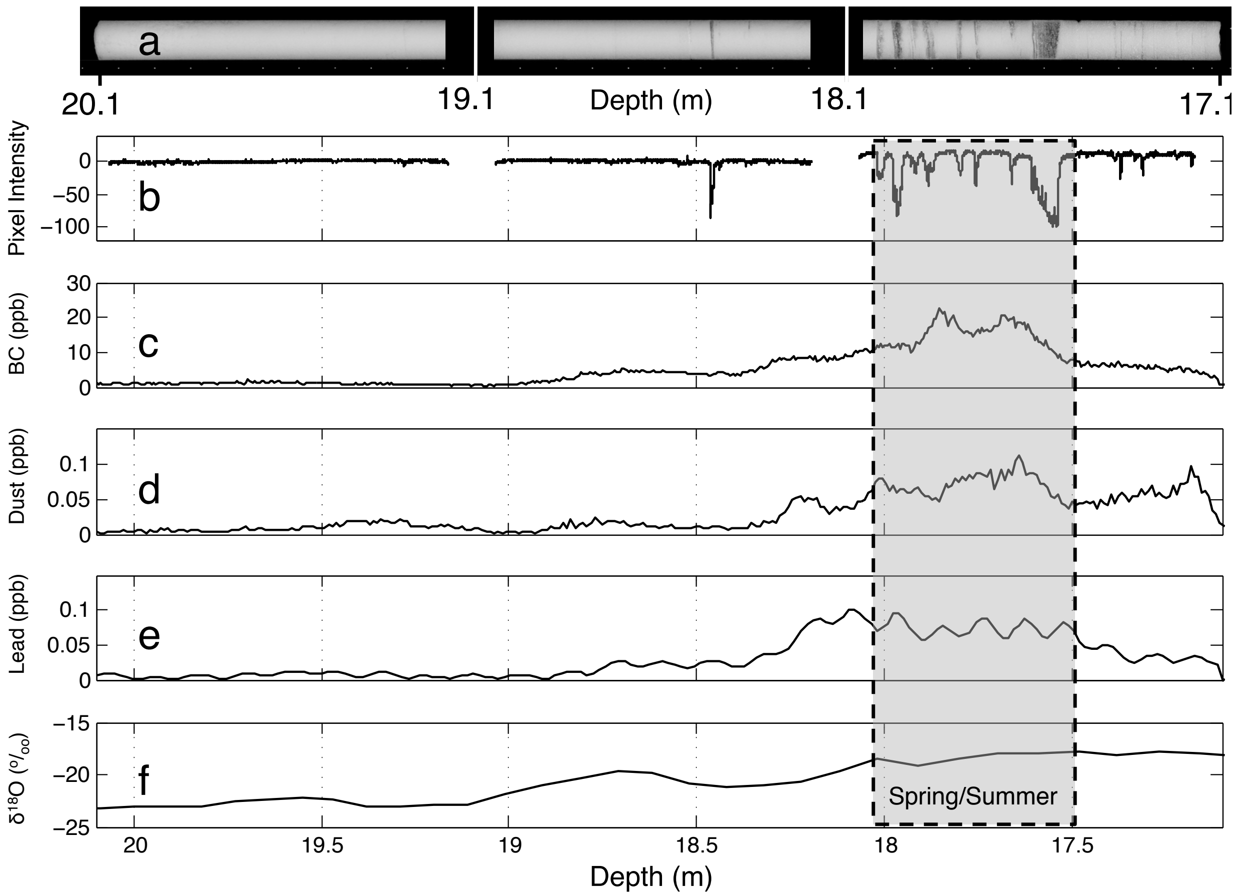

Figure 4. Example section from 17 to 20 m depth in the combatant Col ice core, depicting seasonality in records of a) visual appearance, b) image pixel intensity (melt layers), c) black carbon (BC), d) dust, e) lead, and f) δ^{18}O. All data show lower concentrations/values during winter, gradually increasing to a spring/summer maximum, highlighted by grey box.

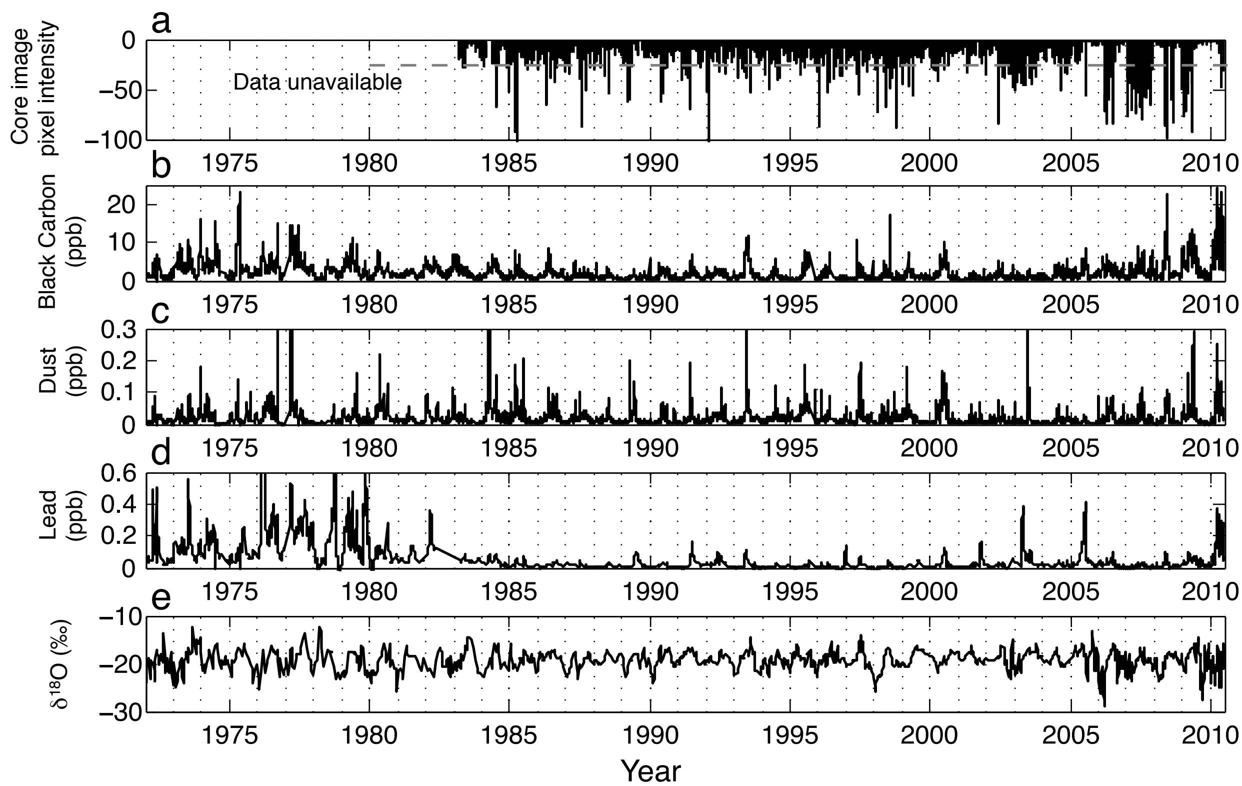

Figure 5. Core image pixel intensity (a), a measure of melt content derived from image brightness (more negative values are dark melt layers which transmit the overhead lighting of the scanner, less negative values are lighter snow or bubbly glacier ice which scatter the overhead lighting of the scanner); black carbon (b); dust (c); lead (d); and $\delta^{18}O$ (e) in the Combatant Col ice core, plotted versus year. For core imaging (a), more transparent glacier ice at depths below the firn-ice transition results in darker images and a noisy record of melt. Based on inspection of the core images, we have added a horizontal dashed line to better highlight melt layers. Values below this line constitute true melt layers. Proper registration of core-images below ~120 m was not possible, but we note that the character of melt in the core does not change below this depth.

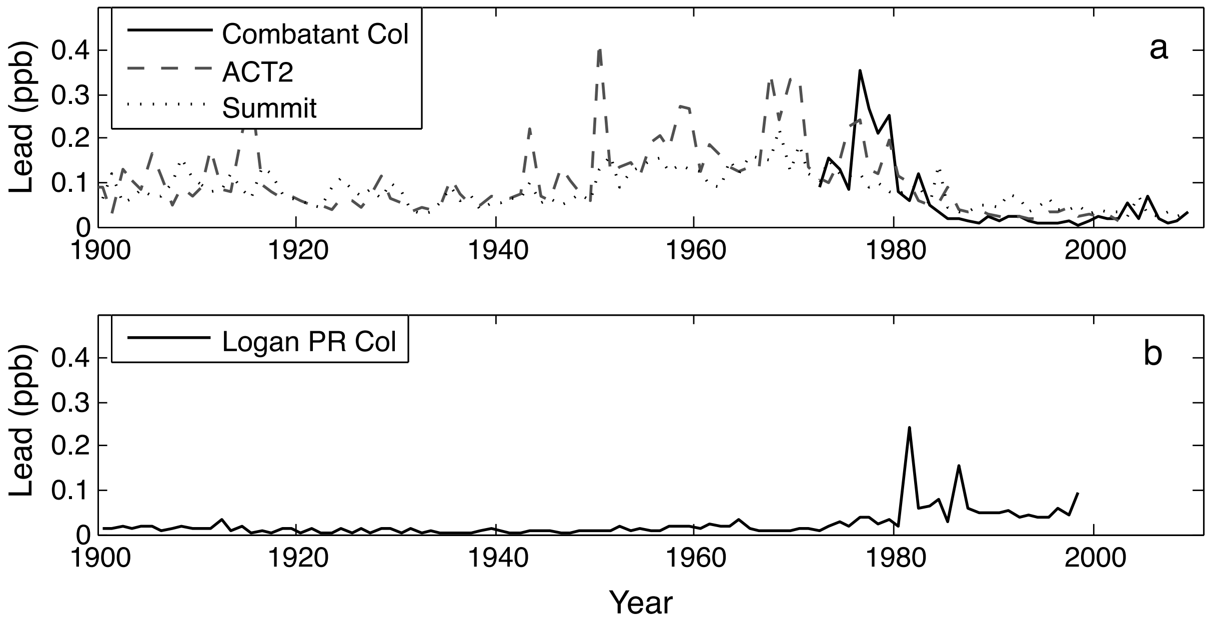

Figure 6. Comparison between Combatant Col annual lead concentrations (a, black line) and ice-core lead records from the Greenland Ice Sheet (a, dotted and dashed lines) and Mt. Logan PR Col (b). Both the Combatant Col and Greenland ACT2 (dashed line) and Summit (dotted line) records show high lead concentrations in the 1970s, followed by sharp decreases in concentration in the early 1980s. In contrast, lead concentrations at Mt. Logan show a steady rise from the 1970s to the most recent years of the record. See Table 1 for location and correlation details.

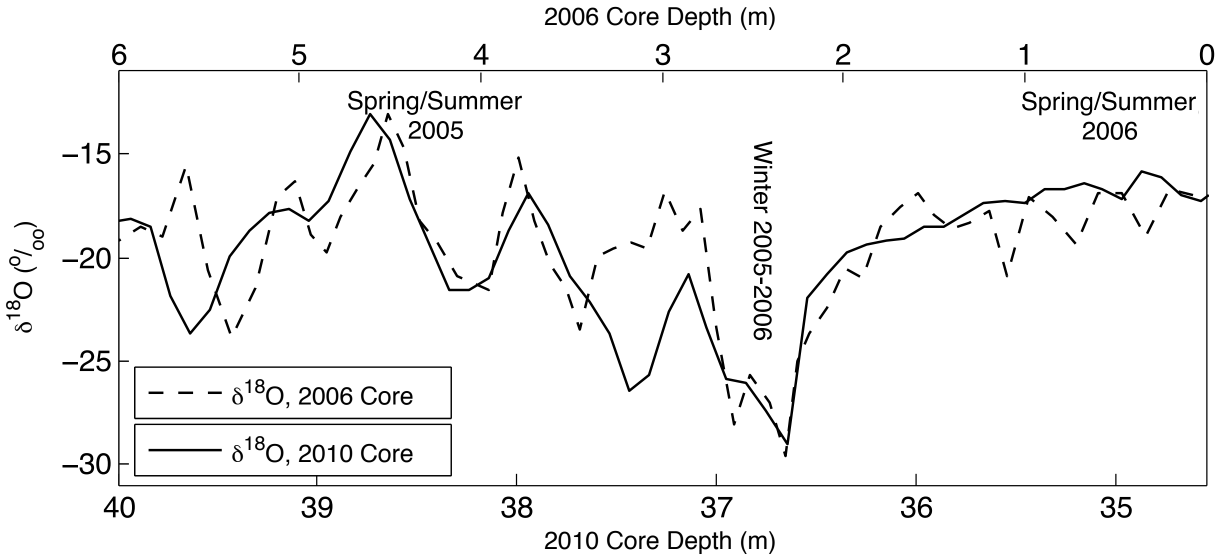

Figure 7. Comparison of $\delta^{18}O$ in the 2006 and 2010 cores. The nearly identical extreme minimum in $\delta^{18}O$, dated independently as winter 2005-2006, demonstrates the preservation of seasonality through firn and into ice.

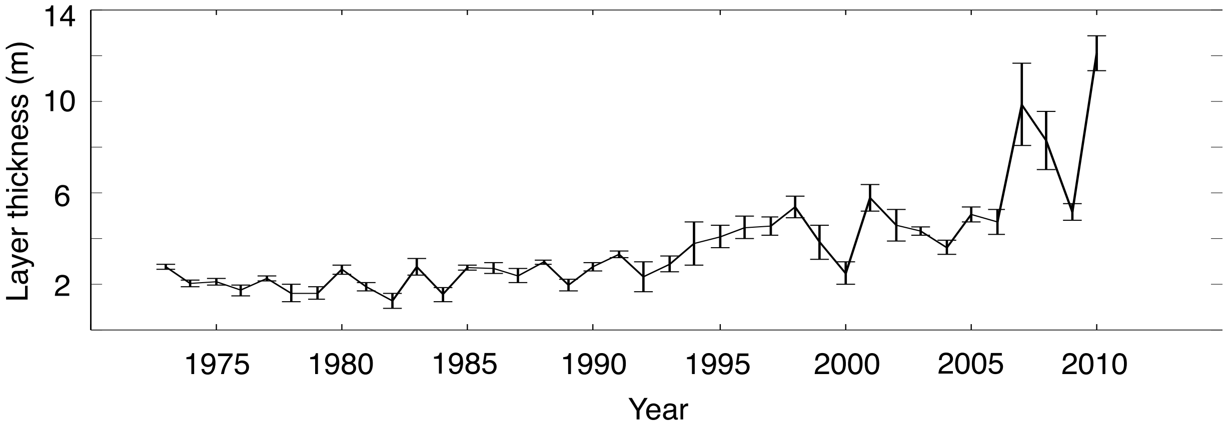

Figure 8. Raw annual layer thickness from the Combatant Col ice core record. Error bars indicate ± one standard error calculated from four agescales (see text for details).

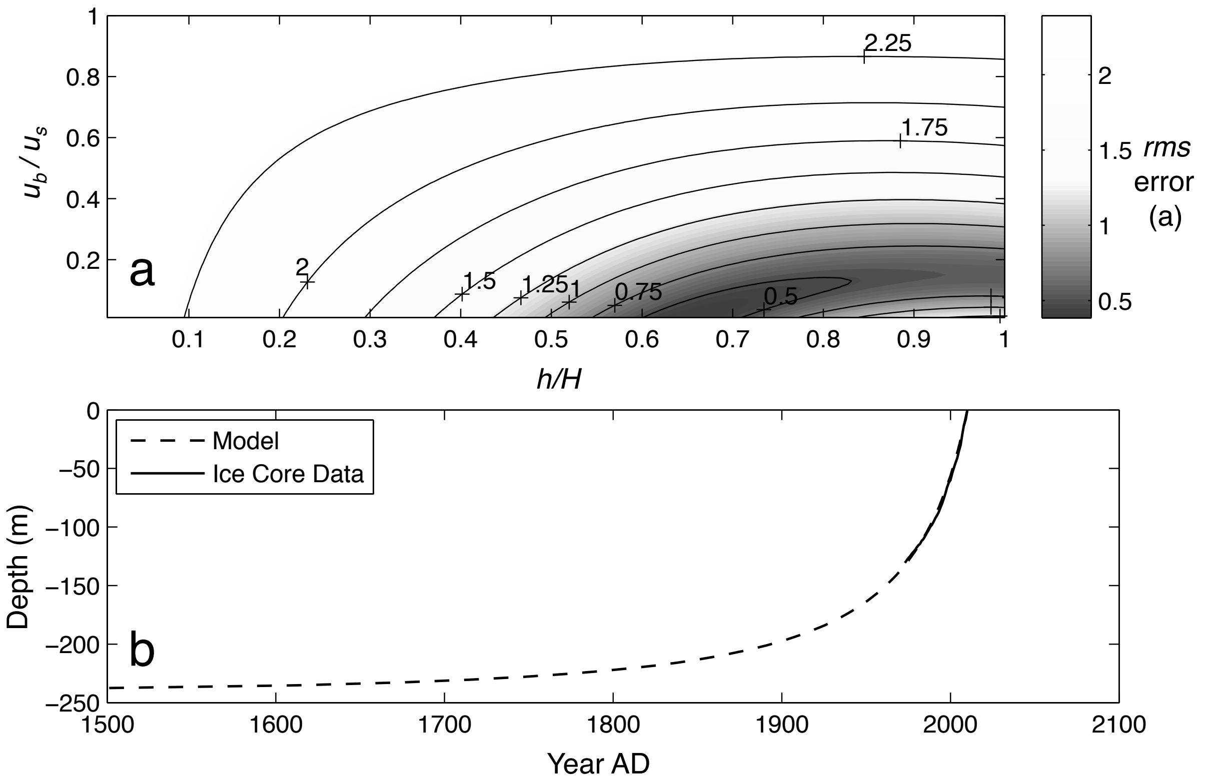

Figure 9. a) Root mean square difference between measured depth-age relationship for the Combatant Col core and that calculated with a Dansgaard-Johnsen flow model for all possible values of h/H and of u_b/u_s ($\dot{b}$ = 7 m a^{-1} and H = 240 m). b) Measured and modeled depth-age relationships, using u_b/u_s = 0, h/H = 0.65, $\dot{b}$ = 7 m a^{-1} and H = 240 m.

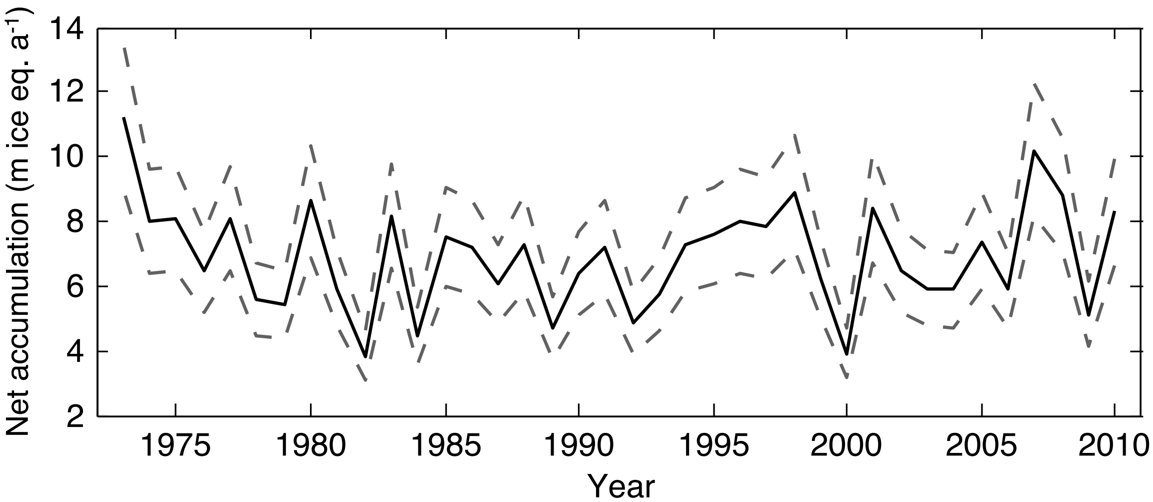

Figure 10. Ice-flow-corrected annual accumulation (m ice-equivalent), with a ± 12% uncertainty threshold marked by the gray dashed lines.

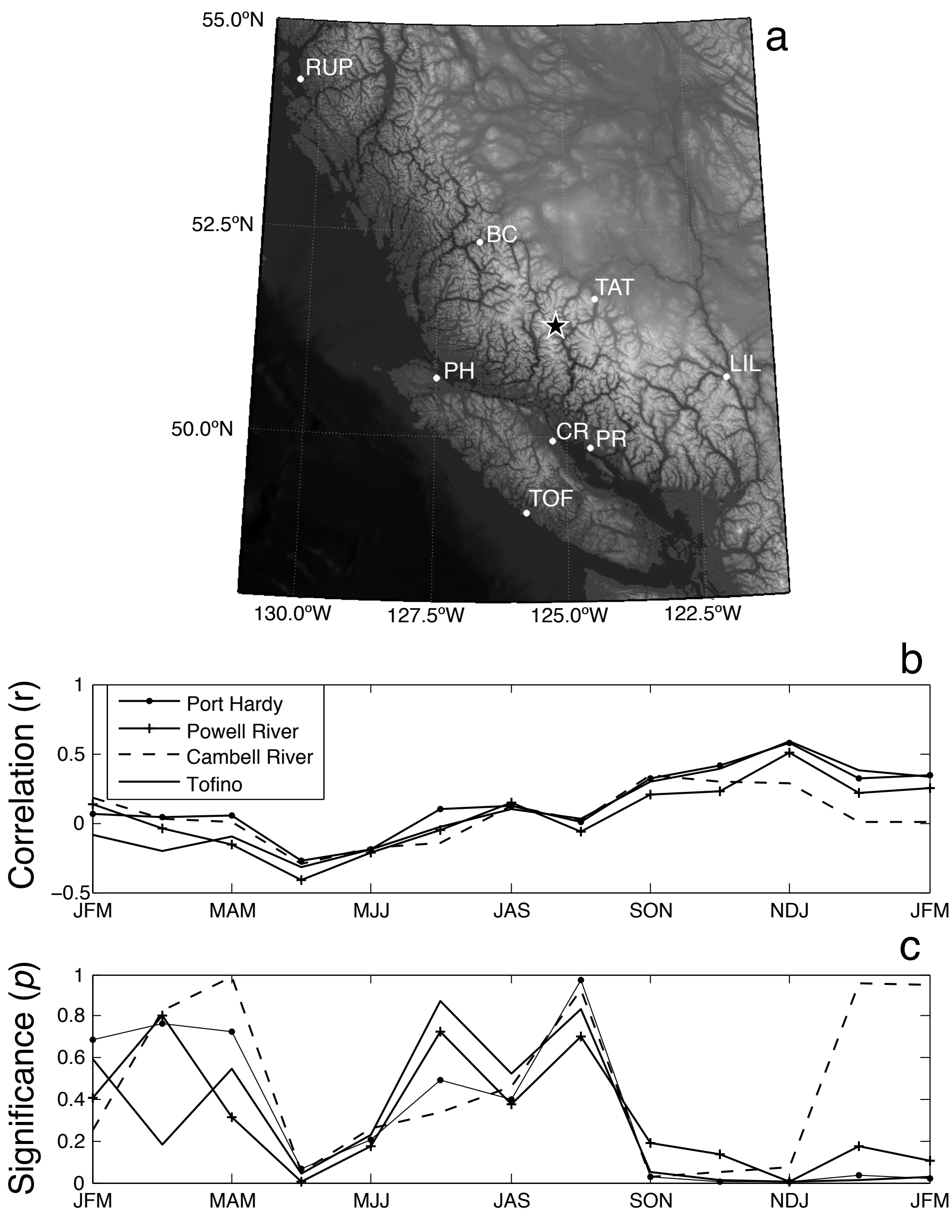

Figure 11. Map (a) shows weather stations used for precipitation data: Port Hardy (PH), Campbell River (CR), Tofino (TOF), Powell River (PR), Prince Rupert (RUP), Bella Coola (BC), Tatlayoko Lake (TAT), and Lillooet (LIL). Combatant Col is starred. b) Correlation (*r*) between 1-year adjusted Combatant Col accumulation timeseries (see text) and seasonal averages of precipitation data from nearby coastal weather stations beginning ± 6 months from JAS of 1973. JFM = January February March, MAM = March April May, MJJ = May June July, JAS = July August September, SON = September October November, NDJ = November December January. c) Significance levels (*p*), indicating that significance of positive correlations between Combatant Col accumulation and weather-station precipitation data are maximized during winter months. Detailed correlation statistics are presented in Table 3.

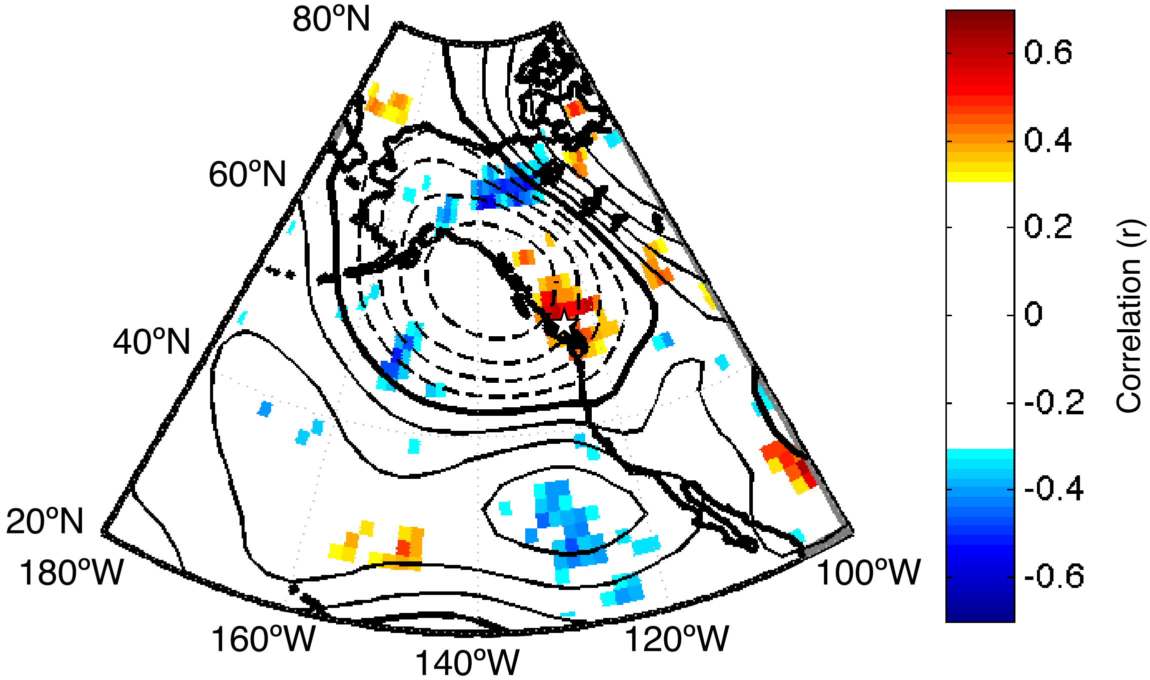

Figure 12. Correlation between Combatant Col annual mean accumulation and ERA-40/ERA-Interim annual precipitation and 500hPa geopotential heights (averaged July through June). Shading indicates correlation (*r*) with precipitation; areas of statistically significant correlation ($p < 0.05$) are colored. Contours (interval 0.1, negative values dashed, zero contour bold, positive values solid) indicate correlation with 500 hPa geopotential height; values <-0.25 and >0.25 are significant at 95%. Combatant Col location is starred.